TARGET TECHNOLOGY LTD.

ATTACHMENT A

SEP TOPIC III-5.A

HIGH ENERGY PIPE BREAKS INSIDE CONTAINMENT

DRESDEN NUCLEAR POWER STATION UNIT 2

DOCKET NO. 50-237

July 27, 1982

Commonwealth Edison Company submitted an Interim Progress Report on June 4, 1982 (Reference 1) which outlined the evaluation criteria, analytical approach, and results which were available at that time. The NRC Draft Evaluation of SEP Topic III-5.A (Reference 2) identified areas where clarification of the methods used and where additional information concerning the assumptions are required for staff acceptance of CECo's evaluation. The five items (B.2, B.7, B.8, B.9, and B.10) identified by the NRC which remain to be resolved are addressed below. The applicable portion of the NRC evaluation item is repeated for clarity.

B.2 "Current criteria require that through-wall leakage cracks be postulated in moderate energy line piping (<200°F and <275 psig). The licensee has not addressed this subject in this SEP topic assessment."

The effects of moderate-energy fluid systems will be evaluated using the following criteria:

1. For piping systems that by plant arrangement and layout are isolated and physically separated and remotely located from systems and components important to safety, through-wall leakage cracks need not be postulated.

2. For piping systems that are located in the same areas as high-energy fluid systems which, by the criteria of Reference 1 Section 3.0 have postulated pipe break locations, through-wall leakage cracks need not be postulated.

3. For piping systems that are located in areas containing systems and components important to safety, but where no high-energy fluid systems are present, through-wall leakage cracks should be postulated at the most adverse location to evaluate the effects of the resulting water spray and flooding. Fluid flow from a crack is based on a circular opening of area equal to that of a rectangle one-half pipe-diameter in length and one-half pipe wall thickness in width.

The environmental effects of pressure, temperature, humidity and flooding are evaluated under SEP Topic III-12, "Environmental Qualification of Safety-Related Equipment" and were not considered in this evaluation. Structural loading effects resulting from fluid flow through the crack, will be considered on safety-related systems, structures and components.

B.7 We have reviewed the information pertaining to the pipe whip and jet impingement interactions with the drywell liner, Reactor Pressure Vessel (RPV) pedestal and biological shield wall. Based on the information submitted in Reference 1, we have determined that the licensee's approach is, in general, acceptable except as follows:

a. Section 4.2 of Reference 1 references Chicago Bridge & Iron Company (CB&I) Test Report (Reference 5). The CB&I test indicates that when a spherical shell segment having a shell thickness of 0.75 inches is loaded over a large enough area, i.e., equivalent to a 14 inch diameter or larger circle, deformation of the plate over 3 inches can occur without failure of the plate segment. Based on this test result, the licensee concludes that for breaks occuring in piping greater than 14 inches in diameter, even if contact occurred with the drywell liner, the amount of liner deformation, as limited by the concrete shield wall, would not result in a liner failure. Accordingly, no acceptable interactions are considered to result with the drywell as a consequence of breaks postulated in piping greater than 14 inches in diameter. However, it should be noted that the CB&I test was performed under essentially static conditions. It is not clear that the test result is also valid for the dynamic loading which would be experienced as a result of pipe whip. In addition, the particular test applies a concentrated load of 235 tons over an area, equivalent to a 14 inch diameter or larger circle. This assumption may not always be valid because the impact area of a 14 inch diameter or larger pipe may be smaller than the assumed area. Thus, our concern is that in the case of applying concentrated dynamic load over a small area the steel plate may be perforated before the deformation is terminated by the concrete shield wall. Therefore, based on the information submitted, we have determined that the licensee has not provided a sufficient justification to use the CB&I test results in its case.

The licensee should select a worst case configuration or other alternative to demonstrate that the impact load or energy produced as a result of postulated pipe break for piping greater than 14 inch diameter does not exceed the load or energy required to penetrate the containment liner and wall. In performing this evaluation with static analysis or static test, the dynamic load factor has to be considered. The licensee can take into account the following considerations:

i. Actual liner thickness with respect to the impact location; and
ii. The combined crack propagation time and break opening time of the pipe may be long enough to depressurize the system such that the whipping pipe could not produce sufficient energy to penetrate the containment wall.

The effects of postulated break locations in lines greater than 14 inches in diameter have been reviewed. Eleven break locations were identified as having interactions with the containment liner. Scaled drawings depicting the movement of the whipping pipe into the containment liner have been prepared. The velocity component normal to the liner at impact is in the range of 10 to 236 feet per second for the above eleven interactions. The lower bound of the normal velocity range results from postulated pipe break locations in lines which have a relatively small gap initially between the piping and the liner with the result that the velocity buildup prior to impact is relatively low.

References 3 and 4 present empirical formulations and test results of missile impact on steel plates. One of the test configurations included a Schedule 40, 12-inch diameter steel pipe weighing 743 lbs. impacting the target panel (3/4 inch thick) end-on at 210 feet per second. In the region of plate impact, the rectangular area unsupported by stiffeners was approximately 3'-6" by 6'-1". Although the test configuration appears to be stiffer than the free standing drywell liner at Dresden 2, the test target plate displacement was greater than 3 inches. As the drywell liner at Dresden 2 is backed up by concrete after a 3 inch displacement of the liner, the pipe test results can be considered to be an upper bound on postulated pipe whip impact on the Dresden 2 liner.

The test velocity for the 12 inch pipe at impact was 210 feet per second. A review of the normal velocities for the eleven postulated pipe whip/liner interactions indicates that ten of the interactions have velocities 114 feet per second or less. The only interaction which is greater than the test velocity of 210 feet per second is for a postulated break location in the feedwater line. The feedwater line appears to make contact with the liner at an 18"x12" reducer in the feedwater line, and the impact for this interaction is considered not to be as severe as the 12 inch pipe end-on impact in Reference 4.

b. The licensee should provide the technical bases for Figure 4-1 of Reference 1 with respect to the energy absorption capacity of containment liner (based on 80 percent penetration).

The modified SRI formula, as presented in References 3 & 4, is used in determining the energy absorption capacity of the containment liner. The formula is given below:

$$\frac{\Delta E}{K_t \sigma_u DT^2} = 4.128 + 0.0967 \frac{W_e}{T} \qquad \text{(Eq. 7-1)}$$

where: $\Delta E = E_1 - E_r$ = Kinetic energy required for performation.

E_1 = Initial kinetic energy of the missile.

E_r = Residual kinetic energy of the missile after penetration (0 in our usage).

K_t = Target energy absorption capacity reduction factor with respect to its ductile fracture temperature - 1.0 at room temperature

σ_u = Ultimate tensile strength of the target material (70,000 psi for containment liner).

D = Outer diameter of missile.

T = Target plate thickness

$W_e = \frac{1}{2}(r_1 + r_2 + r_3 + r_4)C$ = Effective window size.

r_i = Effective crater radius measured from the center of impact along one of the four approximately orthogonal directions; i - 1, 2, 3, 4.

r_c = Full effective crater radius, - 3.6 D if no edge or stiffener is less than this distance from center of impact.

$C = 1/3 \{4 - (\frac{T}{T_o})^2\} \frac{T_o}{T}$ = 1.0 if $T = T_o$

T_o = Actual or calculated thickness for which the missile is just stopped, i.e., $E_r = 0$ (incipient perforation).

This formula was used to calculate the energy absorption capacity of the containment liner for 80% penetration. A plot of the energy capacity for pipe diameters of 2" to 14" was presented in Reference 1 as Figure 4-1.

c. The licensee should clarify the technical bases for Figure 4.2 of Reference 1 and the use of 2500 psi as an upper bound for jet impingement loading on the drywell liner (page 11, Reference 1).

As indicated in Reference 1, Figure 5-1, the work flow for the pipe rupture evaluation is based on a two tier approach. The first tier evaluation (Task 4) is based on conservative analytical criteria which are used to screen the large number of postulated break locations in an efficient manner. Figures 4-1 through 4-6 (Reference 1) are intended to facilitate the accomplishment of this screening process. Figures 4-1 through 4-6 do not represent necessarily the ultimate structural capability of the target. If a target does not pass the Task 4 screening, then the unacceptable interaction is resolved at the second tier level (Task 6) using more sophisticated methods of analysis.

The use of 2500 psi as an upper bound in the nonlinear finite element analysis is based on engineering judgment in order to limit excessive computational expense. An examination of Figure 4-2 (Reference 1), even for a circular loading area equivalent to 20 inches in diameter the curve is already tending toward being asymptotic at 2800 psi. The analysis was performed for circular loading areas as small as 4 inches in diameter in order to cover a full spectrum of target areas. The 2500 psi calculational limit does not imply that actual jet impingement pressures are limited to this value.

The mathematical model (shown in Fig. 7-1) represents a segment of the spherical portion of the containment liner. The center of the loading area is located at the center of the plate. The edges are assumed to be fixed. The dimensions of the model are chosen such that the boundaries are sufficiently far away from the edge of the loading area. Based on small deflection theory, Reference 5 gives the following formula for calculating the minimum distance of the boundary from the edge of the load, for neglecting the boundary conditions.

$$a = R \sin^{-1} (1.65\sqrt{t/R}) \qquad \text{(Eq. 7-2)}$$

where R = Radius of curvature of the spherical shell

t = thickness of the shell

For R = 396" and t = 3/4",

a = 28.46"

for boundary condition effects to be small.

The value of a as calculated from Equation 7-2 is used to determine the size of the generic model.

For the loading areas corresponding to 4", 12", 24" and 36" diameters considered here, the dimensions of the plate used in the finite element model are as follows:

Loading area diameter (inches)	Size of the model (1 in x 1 in)
4	72 x 72
12	96 x 96
24	144 x 144
36	144 x 144

Since the structure, the loading, and the boundary conditions are symmetrical about both x-axis and y-axis (Figure 7-1), symmetrical distribution of the stresses and deflections is expected about x and y-axes. Hence, for the ANSYS finite element analysis, only one-quarter portion of the model located in the first quadrant is considered. The following boundary conditions are assumed in the ANSYS model:

- The displacement parallel to y-axis, i.e., U_y is zero along the boundary y = 0.
- The slope, $\theta_x = \frac{\partial U_2}{\partial y}$ is zero at the boundary, y = 0.

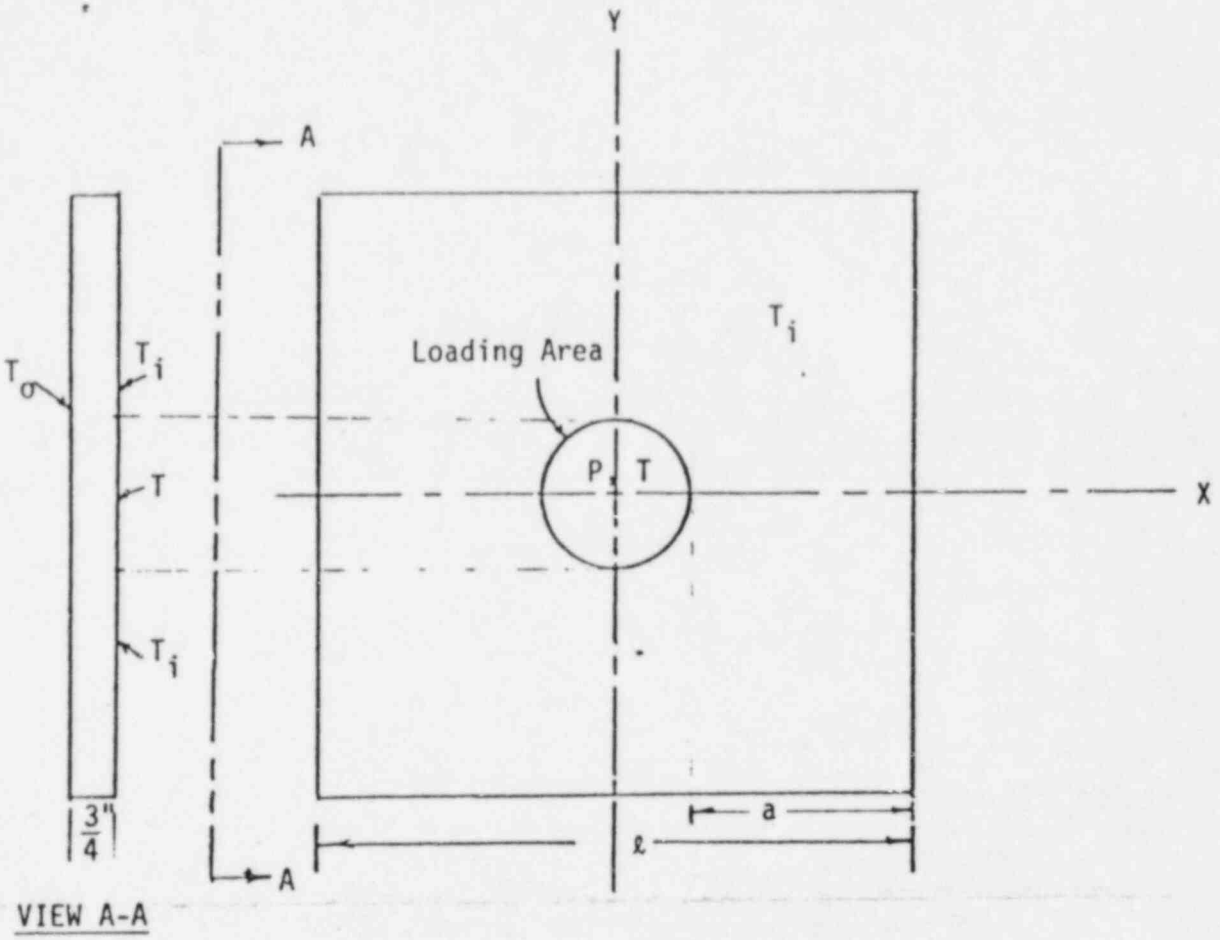

T = Temperature inside impingement area

T_i = Temperature outside impingement area

T_o = Temperature outside drywell

P = Pressure

FIGURE 7-1. MATHEMATICAL MODEL OF THE CONTAINMENT LINER - EVALUATION OF JET IMPINGEMENT EFFECTS

- The displacement parallel to x-axis, U_x is zero along the boundary $x = 0$.
- The slope, $\theta_y = \frac{\partial U_z}{\partial x}$ is zero along $x = 0$.
- The liner is fixed at the remaining two boundaries.

The plastic triangle shell element (STIF 48) in the ANSYS element library has been used in the finite element model of the liner. By using this element, both the membrane stiffness and the bending stiffness in the liner are considered in the analysis. In addition, this element is suitable for analyzing the structure in the plastic domain.

The following loading conditions on the liner were considered in the analysis:

A. Thermal Loads:

In the jet impingement area, the temperature of the liner surface is 575°F. Outside the impingement area, the liner surface is at 165°F. The temperature on the outside surface of the drywell is 100°F.

B. Pressure Loading:

A uniform pressure loading is applied in the jet impingement area. The magnitude of the pressure is gradually increased in steps until either the pressure reached 2500 psi (calculational limit), or the deflection of the liner is about 3".

From ANSYS computer runs, the maximum allowable pressure loadings on the liner for 4", 12", 24" and 36" diameter loading areas were determined. For loading areas corresponding to other diameters, the allowable pressures were computed by interpolation.

d. The licensee should provide the detailed methodology including basic assumptions used in arriving at screening criteria for RPV pedestal and biological shield wall, i.e., the allowable pipe whip loads and maximum allowable jet impingement pressure, for postulated pipe break interactions with RPV pedestal and biological shield wall (Figures 4-3 and 4-4, Reference 1).

The methodology used in arriving at evaluation criteria for postulated pipe break interactions with the RPV pedestal is explained below. The criteria is basically intended to be in the form of curves relating the maximum static equivalent whip loads and jet impingement pressures to the various pipe diameters expected.

Various factors were considered in determining the location of the load. The horizontal load was applied on the outer surface of the pedestal at the location of the haunch in order to include the effects of geometrical discontinuity as well as to be conservative in most cases for overturning stability considerations. Three different loading diameters were considered, viz. 36"Ø, 24"Ø, 12"Ø, along with vertical loads from the Biological Shield Wall and the Reactor Pressure Vessel.

In conformance with the requirements for an initial screening criteria the following conservative assumptions were made:

- All impulsive and impactive loads can be equated to an equivalent static force and the transient nature of the force does not result in adverse dynamic effects.
- Due to the short duration of the jet impingement load the transient temperature effects on concrete can be neglected.
- Pipe diameters less than 2½"Ø will not be considered to affect the RPV pedestal.

Bending stresses were based on the requirements of Chapter 10 of the ACI Code (Ref. 6). The pedestal wall was analyzed in both the hoop and meridional directions. Balanced section conditions were determined using the following equation (Ref. 7).

$$P_b = 0.85 f_c' \beta_1 x_b b + A_s' (f_y - .85 f_c') - A_s f_y$$

$$\text{and } M_b = 0.85 f_c' b\beta_1 x_b (d - 0.5\beta_1 x_b - d'') + A_s' (f_y - .85 f_c')(d - d' - d'') + A_s f_y d''$$

where:

P_b, M_b = balanced section axial load and bending capacities

A_s = area of tension steel

A_s' = area of compression steel

d = section depth

b = section width

f_c' = compressive strength of concrete

f_y = yield strength of steel

β_1 = .85

x_b = $\dfrac{87000d}{f_y + 87000}$

e' = eccentricity of axial load

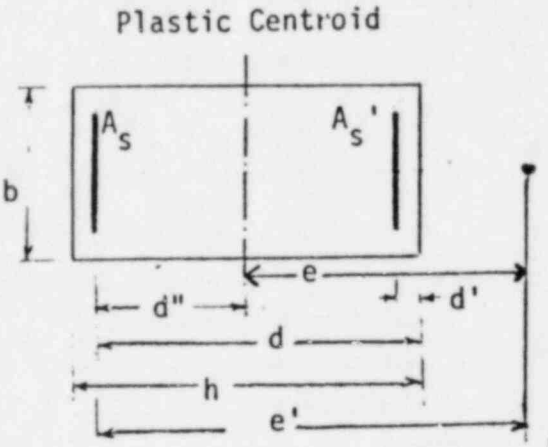

and the rest of the terms are shown in the sketch.

For a section whose capacity is controlled by compression the following equation was used to evaluate the axial load capacity:

$$P_n = bhf_c' \Big/ \left(\frac{3he}{d^2} + \frac{3(d - d')h}{2d^2}\right) + A_s' f_y \Big/ \left(\frac{e}{d-d'} + 0.5\right)$$

For a section whose capacity is controlled by tension the following equation was used to evaluate the axial load capacity:

$$P_n = 0.85 f_c' bd \left\{ \rho + 1 - \frac{e'}{d} + \sqrt{(1 - \frac{e'}{d})^2 + 2\rho \left[(m-1)\left(1 - \frac{d'}{d}\right) + \frac{e'}{d}\right]} \right\}$$

where

P_n = nominal axial load capacity

$\rho = A_s/bd$

and $m = f_y/.85 f_c'$

Shear strength was based on the requirements of Chapter 11 of ACI Code. Stresses were conservatively considered at a section a distance less than 'd', from the face of the load or reaction, where 'd' is the distance from the extreme compression fibre to the centroid of the tension steel. For sections under axial compression (hoop or meridional) the following equation was used to determine shear strength:

$$V_c = \left[1.9\, f_c' + 2500\, \rho_w \frac{V_u d}{M_m}\right] b_w d$$

where

$$M_m = M_u - \frac{N_u(4h - d)}{8}$$

V_c = Nominal shear strength provided by concrete

$\rho_w = A_s/bd$

V_u = Factored shear force at section

$b_w = b$ = section width

M_u = moment corresponding to V_u

and N_u = Factored axial load at section (+ve for compression -ve for tension)

For cases where M_m was negative the following equation was used to determine V_c:

$$V_c = 3.5 \sqrt{f_c'}\, b_w d \sqrt{1 + \frac{N_u}{500 A_g}}$$

where

A_g = gross concrete area

Punching shear evaluation was also based on the requirements of Chapter 11 of ACI Code. The allowable load was calculated using the following formula:

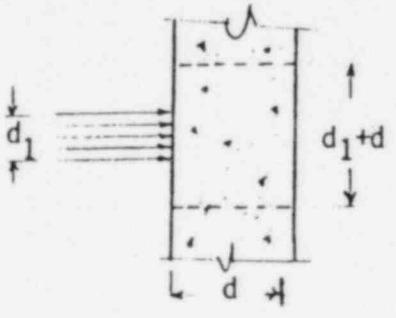

$$P_n = 4\sqrt{f_c'}\ \{\pi(d_1 + d)d\}$$

where P_n = nominal horizontal load

d_1 = diameter of loaded area

and d = depth of concrete section

Overturning stability was based on treating the pedestal as a hollow cylinder. A static analysis was performed to determine the maximum load that the pedestal cross section could allow before developing tension.

Cracked concrete section properties were computed for various cross-sections of the pedestal in both the hoop and meridional directions. These properties were utilized to determine equivalent Young's moduli in these directions.

The RPV pedestal was represented mathematically as an elastic shell. An ANSYS computer model using Element (STIF 25) was developed. The full Pedestal height was required in modelling based on the calculation for decay length from the following equation (Ref. 8):

$$L_c = \pi \left[\frac{a^2 h^2}{3(1 - \gamma_{xs}\gamma_{sx})} \frac{E_x}{E_s} \right]^{\frac{1}{4}}$$

where

L_c = required decay length

a = radius of cylinder

h = thickness of wall

γ_{xs}, γ_{sx} = poisson's ratio in meridional and hoop directions

E_x, E_s = Young's Modulus in meridional and hoop directions

Horizontal loads were applied on these models in the form of a harmonic series of the form:

$$f(\theta) = a_o \sum_{n+1}^{\infty} (a_n \cos n\theta + b_n \sin n\theta)$$

where

$$a_o = \frac{1}{2\pi} \int_{-\pi}^{\pi} f(\theta)\, d\theta$$

$$a_n = \frac{1}{\pi} \int_{\pi}^{\pi} f(\theta) \cos n\theta d\theta$$

b_n = 0 for an even function

The analytical result for the effects of pipe whip and jet impingement on the RPV pedestal were summarized and presented as Figures 4-3 and 4-4 in Reference 1.

The biological shield wall's structural response to pipe whip and jet impingement loads were evaluated using finite element analysis. The magnitude of the applied loading corresponded to the range of expected pipe diameters or jet impingement target areas.

In conformance with the requirements for an initial screening criteria the following conservative assumptions are made:

- All impulsive and impactive loads can be equated to an equivalent static force.
- Due to the short duration of the Jet Impingement, only the loaded area experiences a thermal load, and variations of temperature through thickness and along the surface can be neglected.
- Shielding concrete is capable of transmitting compressive loads from the loaded face to the rear face.

The shield wall was modelled as two thin cylindrical shells connected by axial springs which represented the shielding concrete. It was assumed that the concrete was not capable of transmitting vertical shears between the two plates and hence the choice of a spring-gap element.

The ANSYS elements chosen to model the shield wall are shown schematically in Figure 7-2. The elements were chosen from the ANSYS element library and a list of elements along with their salient features is given in Table 7-1.

Evaluations were based on the more conservative of the following criteria:

(1) An average deflection under the loaded area of 4".
(2) A maximum strain of up to 50 percent of ultimate strain.

An examination of the results indicated that the strains under applied loads were much lower than the limitation, and the deflection criteria governed in all cases. Overall stability computations were performed to determine the capacity of anchoring mechanisms at the bases into the RPV Pedestal.

The analytical results for the effects of pipe whip and jet impingement on the sacrificial shield wall were summarized and presented as Figures 4-5 and 4-6 in Reference 1. These figures are used in screening interactions with the sacrificial shield wall as part of the Task 4 activity.

FIGURE 7-2. SCHEMATIC SKETCH OF ANSYS ELEMENTS

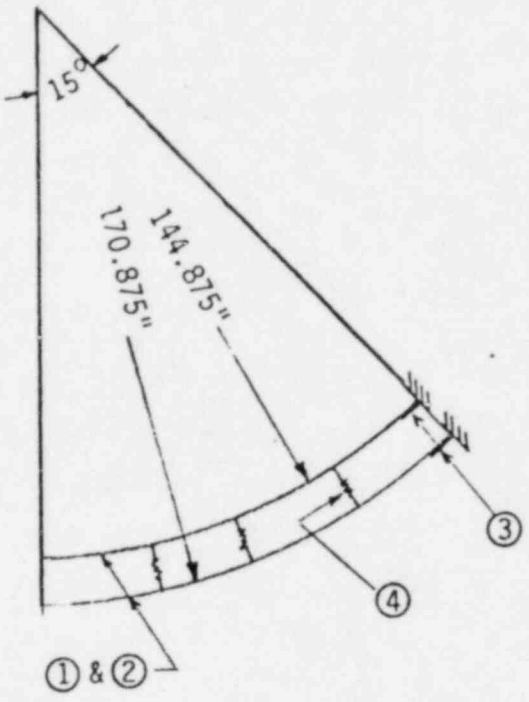

TABLE 7-1. ANSYS ELEMENTS FOR SHIELD WALL MODELLING

ELEMENT NO.	ANSYS ELEMENT NO.	DESCRIPTION	ANSYS FEATURES
1	STIF 43	1/4" plate, front & rear	Rectangular Shell Element. Capabilities in the Elastic range of material properties only. Six DOF's at each node.
2	STIF 48	1/4" plate, front & rear	Triangular Shell Element. Permits properties in the Plastic range. Six DOF's at each node. This element enables the use of nonlinear isotropic material.
3	STIF 43	Flange of W27x177	See Element No. 1
4	STIF 40	Concrete in compression only	Combination element with a gap. This element enables the use of only compression loading with no shear transfer, for modeling the concrete fill.

B.8 In considering the damage criteria (Section 4.5 of Reference 1), the licensee has used the assumption that a jet or whipping pipe is considered to inflict no damage on other pipes of equal or greater size and equal or greater thickness. It is the staff's position (Reference 7) that the effects of jet impingement should be considered and evaluated regardless of the ratio of impinged and postulated broken pipe sizes.

The jet thrust force acting on the end of a whipping pipe may be represented by a steady state function if a static model is used in the subsequent pipe motion analysis. The function should have a magnitude not less than

$$T = KpA \qquad \text{(Eq. 8-1)}$$

where

p = system pressure prior to pipe break

A = pipe break area

K = thrust coefficient.

For the case of a ruptured pipe that is initially in contact with the target pipe, the equivalent static force on the target pipe can be conservatively represented by

$$F_{eq.} = (2.0)\ (KpA) \qquad \text{(Eq. 8-2)}$$

where the dynamic load factor is conservatively selected as 2.0.

The jet impingement force emanating from the end of a broken pipe can be also conservatively represented by Equation 8-1. The equivalent static force on the target pipe as a result of jet impingement can also be conservatively represented by Equation 8-2.

It can be concluded therefore that the equivalent static force on the target pipe resulting from either pipe whip effects or jet impingement effects is of the same magnitude for the above case. Consider next, the case of a ruptured pipe that is separated by a gap from the target pipe. The jet thrust force will be acting on the whipping pipe as in the first case. However, because the whipping pipe is being accelerated through a gap prior to contact with the target pipe, an inertia force component will also be present. The equivalent static force due to pipe whip in the presence of a gap can be expressed as

$$F_{eq.} = (2.0)\ (KpA + \text{Inertia Force Component}) \qquad \text{(Eq. 8-3)}$$

where a dynamic load factor of 2.0 is assumed.

Equation 8-2 is an upper bound on the equivalent static load resulting from jet impingement effects. It is equal to the equivalent static load from pipe whip (Equation 8-2) or less than the equivalent static load from pipe whip (Equation 8-3), depending on whether the gap between the ruptured pipe is zero or some finite distance.

The NRC position as stated in Standard Review Plan 3.6.2 is that an unrestrained whipping pipe will not cause unacceptable damage in impacted pipes of the same or greater nominal pipe size and with the same or greater wall thicknesses. On the basis of the results of Equations 8-2 and 8-3 which indicate that the equivalent static force from pipe whip is equal to or greater than the equivalent static force from jet impingement, it is concluded that the same rule which is applicable to pipe whip should also be applicable to jet impingement considerations.

Target pipe interactions from pipe whip or jet impingement are evaluated using Equation 4-3 (Reference 1) if the relationships

$$d_T \geq d_W \text{ and } t_T \geq t_W$$

where:

d_T = diameter of target pipe
d_W = diameter of pipe with postulated break location
t_T = wall thickness of target pipe
t_W = wall thickness of pipe with postulated break location

are not satisfied.

B.9 In determining the acceptability of target pipe (Section 4.3.2 of Reference 1), the licensee has used a criterion that the limiting factor for an applied equivalent static load is that the resulting strain in the target pipe material does not exceed 45 percent of the minimum ultimate uniform strain of the material at the appropriate temperature. This criteria is acceptable for avoiding cascading pipe breaks. However, some piping systems are required to deliver certain rated flow and should be designed to retain dimensional stability when stressed to the allowable limits associated with the emergency and faulted conditions, i.e., the functional capability of the piping is required to be demonstrated. The licensee should provide justification to assure that the target piping will remain functional as a result of jet impingement and pipe whip interactions.

Plastic hinge formation of the target pipe is of a very localized nature and the zone of plasticity is limited essentially to the hinge location. It is therefore possible to achieve strain levels approaching 45 percent of the minimum uniform ultimate strain of the material in a localized region without affecting the overall deformation or functionality of the target pipe.

A parametric study covering a range of geometric and load parameters was performed using the ANSYS finite element program. The nonlinear dynamic analysis results indicated the coexistence of large localized strain levels and small global deformations. The above conclusion is illustrated by the following numerical results from the ANSYS computer program.

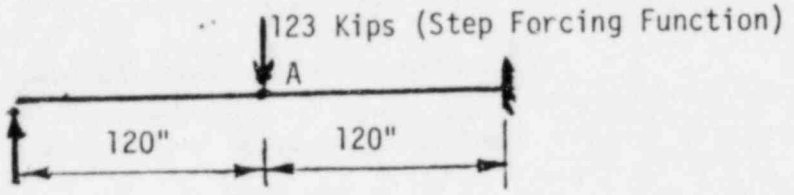

Target pipe properties used were as follows:

Pipe = 16 inch diameter - Schedule 40
Wall Thickness = 0.5 inches
σ_y = 35,000 psi

The plastic hinge which formed at point A (point of load application) reached a strain level of 45 percent of the minimum uniform ultimate strain of the material. The downward displacement of point A was 1.643 inches with an angle of rotation at the support of 0.78 degrees.

It should be noted that Section 4.3.2 (Reference 1) was developed as a conservative screening criteria for application in the Task 4 activity. Interactions which are determined not to satisfy this conservative criteria are evaluated in Task 6 using sophisticated analytical methods as appropriate on a case-by-case basis.

B.10 The licensee's approach for the alternative safety assessment for selected high energy pipe break locations using fracture mechanics analysis is not completely consistent with the staff guidance on the subject as described in Appendix 1 to Attachment to Enclosure 2. For example, the licensee did not address the detectability requirements. The staff recommends that the licensee consider the staff guidance as provided in Enclosure 2 for resolution of unresolved interactions.

The staff guidance for the alternative safety assessment of high energy pipe break locations using fracture mechanics analysis is based on satisfying the requirements for detectability, integrity and consideration of extreme loading conditions. The approach proposed by CECo for satisfying the integrity and extreme loading condition requirements reflects the guidance provided in Reference 2 (Appendix 1 to Attachment to Enclosure 2).

CECo's approach for satisfying the detectability requirement is based on the leak-before-break concept and consists of the following steps:

1. The initial crack size is based on a Code allowable surface defect.

2. Crack growth is based on a fatigue mechanism.

3. The end-of-life crack size reflects the growth potential of the initial crack under expected operating conditions.

4. The end-of-life crack size is compared to the critical crack length in order to establish the margin of safety.

5. If the end-of-life crack becomes a through-the-wall crack, then the leakage for this crack length is calculated.

6. Calculate the leakage from a through-the-wall crack which is of critical length and establish the margin of safety on leakage from the critical length crack as compared to the leakage from the end-of-life crack.

7. For the specific postulated break location, determine what the current capability to detect leakage is and compare this capability to the leakage from the critical length crack. Provide additional leakage detection capability as required to ensure that the margin of safety on leakage detection is greater than 100 percent.

REFERENCES

1. Letter from T.J. Rausch (CECo) to D.M. Crutchfield (NRC), dated June 4, 1982, Attachment 1 - Report, "Dresden 2 Nuclear Power Station SEP Topic III-5.A, High Energy Pipe Break Inside Containment Interim Progress Report," dated May 18, 1982.

2. Letter from D.M. Crutchfield (NRC) to L. DelGeorge (CECo), dated June 29, 1982, Enclosure 1, "SEP Draft Evaluation of Effects of Pipe Break on Structures, Systems and Components Inside Containment Topic III-5.A Dresden 2 Nuclear Power Station."

3. "Report of the ASCE Committee on Impactive and Impulsive Loads" - Civil Engineering and Nuclear Power, Volume V, September, 1980.

4. "Special Criteria Developed for the Design and Analysis of Floating Nuclear Plant Containment Structures," Tsai, J.C., Orr, R.S., Transactions of the 4th International Conference on Structural Mechanics in Reactor Technology, Vol. J(a), August 19, 1977.

5. Roark, R.J., and Young, W.C., Formulas for Stress and Strain, 5th Edition, McGraw-Hill, 1975.

6. "Code Requirements for Nuclear Safety Related Concrete Structures," ACI 349-80

7. Salmon and Wang, Reinforced Concrete Design, Intext Press, 1973.

8. Kraus, H., Thin Elastic Shells, John Wiley, June, 1967.